

LETTER • OPEN ACCESS

# Satellite-derived foresummer drought sensitivity of plant productivity in Rocky Mountain headwater catchments: spatial heterogeneity and geological-geomorphological control

Recent citations

- [Remote Sensing-Informed Zonation for Understanding Snow, Plant and Soil Moisture Dynamics within a Mountain Ecosystem](#)  
Jashvina Devadoss *et al*

To cite this article: Haruko M Wainwright *et al* 2020 *Environ. Res. Lett.* **15** 084018

View the [article online](#) for updates and enhancements.

# Environmental Research Letters



## LETTER

### OPEN ACCESS

RECEIVED  
4 January 2020

REVISED  
17 April 2020



ACCEPTED FOR PUBLICATION  
4 May 2020

PUBLISHED  
21 July 2020

Original content from this work may be used under the terms of the [Creative Commons Attribution 4.0 licence](#). Any further distribution of this work must maintain attribution to the author(s) and the title of the work, journal citation and DOI.



## Satellite-derived foresummer drought sensitivity of plant productivity in Rocky Mountain headwater catchments: spatial heterogeneity and geological-geomorphological control

Haruko M Wainwright<sup>1</sup> , Christoph Steefel<sup>2</sup>, Sarah D Trutner<sup>3</sup>, Amanda N Henderson<sup>4</sup>, Efthymios I Nikolopoulos<sup>5</sup>, Chelsea F Wilmer<sup>6</sup>, K Dana Chadwick<sup>1,7</sup> , Nicola Falco<sup>1</sup>, Karl Bernard Schaettle<sup>8,9</sup>, James Bentley Brown<sup>10</sup>, Heidi Steltzer<sup>11</sup>, Kenneth H Williams<sup>1,4</sup>, Susan S Hubbard<sup>1</sup> and Brian J Enquist<sup>12</sup>

- <sup>1</sup> Climate and Ecosystem Sciences Division, Lawrence Berkeley National Laboratory, 1 Cyclotron Road, MS 74R-316C, Berkeley, CA 94720-8126, United States of America
- <sup>2</sup> Lawrence Berkeley National Laboratory, 988 Belmont Terrace Unit 10, Sunnyvale, CA 94086, United States of America
- <sup>3</sup> Colorado School of Mines, 1500 Illinois St, Golden, CO 80401, United States of America
- <sup>4</sup> Rocky Mountain Biological Laboratory, PO Box 519, Crested Butte, CO 81224, United States of America
- <sup>5</sup> Department of Mechanical and Civil Engineering, Florida Institute of Technology, 150 W. University Blvd, Melbourne, FL 32901, United States of America
- <sup>6</sup> Department of Ecosystem Science and Sustainability, Colorado State University, Fort Collins, Colorado 80523-1476, United States of America
- <sup>7</sup> Department of Earth System Science, Stanford University, 473 Via Ortega, Stanford, CA 94305, United States of America
- <sup>8</sup> Chemical and Biomolecular Engineering, University of California, Berkeley, United States of America
- <sup>9</sup> Gilman Hall University of California Berkeley, CA 94720-1462, United States of America
- <sup>10</sup> Environmental Genomics and Systems Biology, Lawrence Berkeley National Laboratory, 1 Cyclotron Road, MS 74R-316C, Berkeley, CA 94720-8126, United States of America
- <sup>11</sup> Department of Biology, Fort Lewis College, Durango, Colorado 81301, United States of America
- <sup>12</sup> Department of Ecology and Evolutionary Biology, University of Arizona, Tucson, AZ 85721, United States of America

E-mail: [hmwainwright@lbl.gov](mailto:hmwainwright@lbl.gov)

**Keywords:** random forest, Rocky Mountains, NDVI, foresummer drought sensitivity

Supplementary material for this article is available [online](#)

### Abstract

Long-term plot-scale studies have found water limitation to be a key factor driving ecosystem productivity in the Rocky Mountains. Specifically, the intensity of early summer (the ‘foresummer’ period from May to June) drought conditions appears to impose critical controls on peak ecosystem productivity. This study aims to (1) assess the importance of early snowmelt and foresummer drought in controlling peak plant productivity, based on the historical Landsat normalized-difference vegetation index (NDVI) and climate data; (2) map the spatial heterogeneity of foresummer drought sensitivity; and (3) identify the environmental controls (e.g. geomorphology, elevation, geology, plant types) on drought sensitivity. Our domain (15 × 15 km) includes four drainages within the East Water watershed near Gothic, Colorado, USA. We define foresummer drought sensitivity based on the regression slopes of the annual peak NDVI against the June Palmer Drought Severity Index between 1992 and 2010. Results show that foresummer drought sensitivity is spatially heterogeneous, and primarily dependent on the plant type and elevation. In support of the plot-based studies, we find that years with earlier snowmelt and drier foresummer conditions lead to lower peak NDVI; particularly in the low-elevation regions. Using random forest analysis, we identify additional key controls related to surface energy exchanges (i.e. potential net radiation), hydrological processes (i.e. microtopography and slope), and underlying geology. This remote-sensing-based approach for quantifying foresummer drought sensitivity can be used to identify the regions that are vulnerable or resilient to climate perturbations, as well as to inform future sampling, characterization, and modeling studies.

## 1. Introduction

Ecosystems in headwater catchments are important for water resources, because they influence hydrology through evapotranspiration (ET) and nutrient cycling (e.g. Lukas *et al* 2015, Maxwell and Condon 2016). Recent global-climate-model ensembles predict increased temperature and earlier snowmelt in western North America (Higgins and Shi 2001, Diefenbaugh *et al* 2013). Additionally, some studies predict reduced spring precipitation and increased late-summer monsoon precipitation in the future (Seth *et al* 2011). Together, these changes would increase the length of time between snowmelt and summer monsoon, or the ‘foresummer’ part of growing seasons (Rauscher *et al* 2008, Swain and Hayhoe 2015). Low snowpack years with earlier snowmelt would expose plants to potentially longer and drier periods before the onset of monsoonal precipitation. Combined with predicted increasingly warmer temperatures, this foresummer period could become more drought-like.

Recently, (Sloat *et al* 2015) documented the importance of this *foresummer drought* period by combining a watering manipulation experiment with 11 years of long-term monitoring data at the Rocky Mountain Biological Laboratory (RMBL) in Gothic, Colorado, USA. They found that peak and cumulative net ecosystem productivity (NEP) is negatively correlated with the severity of drought conditions in the primary growing season (June). They concluded that NEP will not increase in the future, despite the increase in temperature and longer growing seasons. This is consistent with other studies that reported water limitation of ecosystem productivity in the Rocky Mountain regions (e.g. Lamanna 2012, Williams *et al* 2012, Harte *et al* 2015) and in the western USA (Berner *et al* 2017). These regions are thus in contrast with other regions where water is not a limiting factor, and therefore early snowmelt lengthens the growing season, and increases the rate of peak and cumulative ecosystem productivity (e.g. Euskirchen *et al* 2006; Ernakovich *et al* 2014).

Here, we address the key challenge of scaling up such plot-scale experiments in order to quantify overall ecosystem and/or plant productivity at the scale of watersheds. Ecosystems in mountainous regions are particularly heterogeneous, influenced by steep and complex terrains. In these systems, plant types can vary on a spatial scale of 50–100 m (Zimmermann and Kienast 1999). Slope and aspect affect solar radiation, which in turn influences energy balance and soil moisture (Körner 2007). Soil moisture is also affected by plant types, soil types, and other factors (e.g. Mohanty *et al* 2000). In addition, snow accumulation and melting—which leads to infiltration and provides a critical water storage mechanism for ecosystems in the growing season (Harte *et al* 2015, Sloat *et al* 2015)—are extremely heterogeneous in

mountainous regions (Anderson *et al* 2014, Painter *et al* 2016).

In this study, we propose a new sensitivity metric for the Rocky Mountain region, and to map this sensitivity using historical satellite and climate data. The historical records of satellite datasets are valuable in evaluating the long-term trends and responses of ecosystems to climate variations, and also in inferring their future responses to changing climate (e.g. Zhao and Running 2010, Seddon *et al* 2016, Knowles *et al* 2017, 2018, Stocker *et al* 2019, Dong *et al* 2019). Given the water-resource limitation in this region during early growing seasons, herein we define *foresummer drought sensitivity* as the sensitivity of peak plant productivity to foresummer drought conditions. We then quantify this sensitivity based upon the historical records of the Landsat-derived normalized difference vegetation index (NDVI) at 30 m resolution, which is known to be strongly correlated with plant productivity (e.g. Tucker *et al* 1985, De Jong *et al* 2011, Dong *et al* 2019). We represent the drought condition based on the June Palmer Severity Drought index (PSDI) in the same manner as (Sloat *et al* 2015). In contrast to other satellite-based studies, our drought sensitivity is based on plot-scale experiments and the associated system understanding shown in (Sloat *et al* 2015). In addition, we use a machine learning approach to investigate environmental controls on spatially heterogeneous sensitivity, including elevation, geomorphology, and geology, using publicly available spatial datasets. Such data-driven analysis provides useful insights into underlying processes, enhances our ability to predict future trajectories, informs mechanistic ecohydrological models, and also facilitates site characterization and sampling plans.

## 2. Materials and methods

### 2.1. Study area

We consider an approximately 15-km-by-15-km domain near Gothic, Colorado, USA (figure 1). (Hubbard *et al* 2018) provides a detailed site description. The domain is part of the Elk Mountain Range in the Rocky Mountains, with elevation ranging from ~2800 m to ~4000 m (figure 1(a)). The major land cover types are rock outcrop (12%), evergreen forest (29%), deciduous forest (18%), and grassland (30%; figure 1(b), NLCD 2011). The domain includes four drainages (East River, Washington Gulch, Slate River and Coal Creek) and four of the five experimental plots used in (Sloat *et al* 2015).

Historically, snow precipitation starts in October to November, and the first bare-ground date ranges from May to June. (Carroll *et al* 2018) analyzed the peak snow distribution in April, 2016 based on the NASA Airborne Snow Observatory, and found that the snow depth varies, ranging from 0 to 2.36 meters depending on the elevation, aspect and plant cover type. At the Butte Snow Telemetry (SNOTEL) station

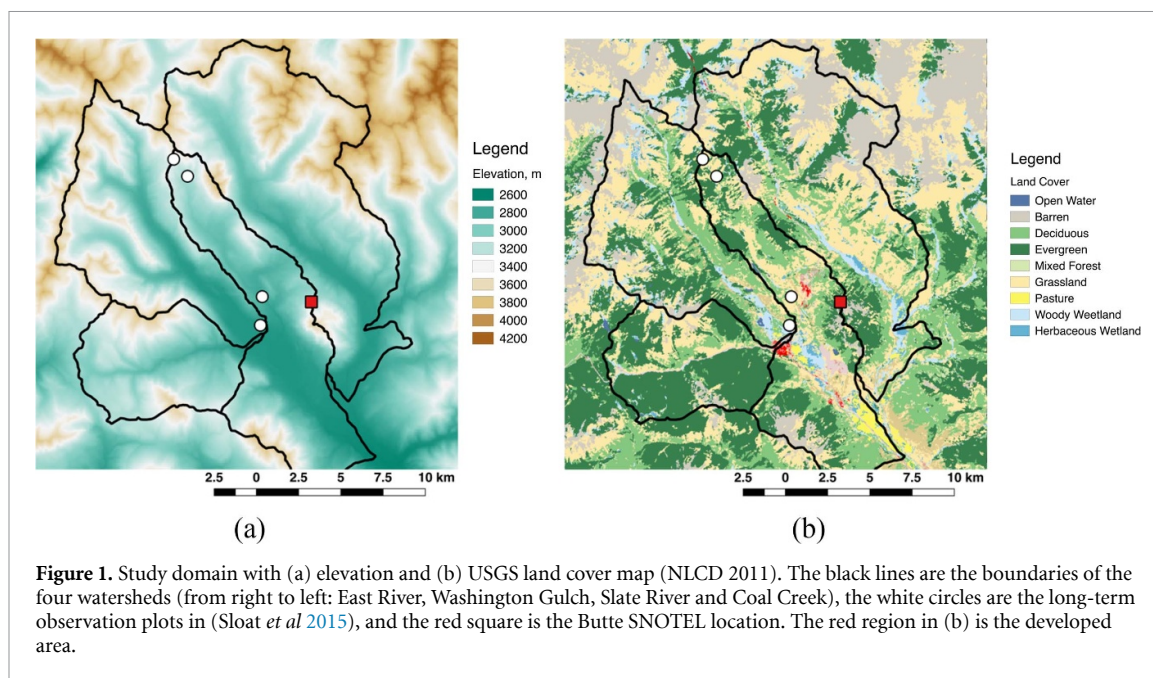


**Figure 1.** Study domain with (a) elevation and (b) USGS land cover map (NLCD 2011). The black lines are the boundaries of the four watersheds (from right to left: East River, Washington Gulch, Slate River and Coal Creek), the white circles are the long-term observation plots in (Sloat *et al* 2015), and the red square is the Butte SNOTEL location. The red region in (b) is the developed area.

(figure 1), the historical average of peak snow-water-equivalent and first bare-ground date are 400.5 mm and May 21st, respectively.

## 2.2. Palmer drought index and climate data

We used the June PDSI of Colorado Division 2 from NOAA ([www.cpc.ncep.noaa.gov/products/analysis\\_monitoring/cdus/palmer\\_drought/](http://www.cpc.ncep.noaa.gov/products/analysis_monitoring/cdus/palmer_drought/)) to represent foresummer drought conditions. PDSI is computed based on precipitation, temperature, and division constants (such as soil water capacity). Although the limitations of PDSI have been recognized (Alley 1984, Dai *et al* 2004, Trenberth *et al* 2014), it is still the most widely used index for drought conditions (e.g. Dong *et al* 2019). Note that although the data source is different from (Sloat *et al* 2015), we assume that the general climate variability is captured similarly by both PDSIs. In addition, we evaluated other drought indices (text S1): Standardized Precipitation Index (SPI; McKee *et al* 1993), and Standardized Precipitation Evapotranspiration Index (SPEI; Beguería *et al* 2010, Vicente-Serrano *et al* 2012).

We also used snowmelt timing (i.e. first bare-ground date) and June mean air temperature from the Butte SNOTEL station (elevation 3097 m; [www.wcc.nrcs.usda.gov/snow/](http://www.wcc.nrcs.usda.gov/snow/)). We used the homogenized SNOTEL temperature data provided by Oyler (*et al* 2015). All the data values are included in table S1 and figure S1 (available online at [stacks.iop.org/ERL/15/084018/mmedia](http://stacks.iop.org/ERL/15/084018/mmedia)). We also confirmed that the average June precipitation is significantly lower than the other months (table S2).

## 2.3. Annual peak NDVI and sensitivity measures

Using Google Earth Engine (GEE; <https://earthengine.google.com/>), we processed Landsat 5 surface reflectance datasets over 19 years (1992–2010).

These images were processed, including the atmospheric correction by the LEDAPS method (<http://ledaps.nascom.nasa.gov/>). We computed NDVI at each pixel, and annual peak NDVI (i.e. the maximum value at each pixel) in each year. Finally, we downloaded these annual peak NDVI images for further analysis. Since two Landsat paths overlapped over this domain, the repeat cycle was 8 d, which contributed to minimizing the effect of cloud coverage.

We first extracted peak NDVI at the pixels corresponding to the observation plots in (Sloat *et al* 2015) to investigate the relationship between peak NDVI and June PDSI, snowmelt timing, and June mean air temperature. We then defined the foresummer drought sensitivity as the slope of peak NDVI as a linear function of June PDSI. The slope represented the change in peak NDVI given the change in June PDSI. We also computed the average and standard deviation (SD) of annual peak NDVI at each pixel. In addition, we analyzed the relationship between NDVI and leaf area index (LAI) based on the ground-based measurements collected in 2019 (text S2 and figure S2).

## 2.4. Random forest analysis for environmental controls on drought sensitivity

We investigated key controls on foresummer drought sensitivity, based on other spatial data layers used in the hydrological modeling study within this domain (Pribulick *et al* 2016, Foster and Maxwell 2019). The Random Forest (RF) method is a machine-learning method developed by (Breiman 2001) to predict responses based on mixed numerical and categorical predictors, and to identify important predictors for given responses (Hastie *et al* 2001). RF generates a large number of regression trees from bootstrapped subsampled data, and averages over all the

trees. RF is known to work well with correlated predictors similar to ridge regressions (Hastie *et al* 2001). In environmental applications, (Bachmair and Weiler 2012) used RF for identifying key controls on hillslope hydrological dynamics.

We defined a regression of foresummer drought sensitivity as a function of environmental variables. Using Topotoolbox (Schwanghart and Kuhn 2010), we computed topographic metrics based on the digital elevation model (DEM) from the National Elevation Dataset (30 m resolution, U.S Geological Survey 2002), including slope, topographic wetness index (TWI), bedrock-weighted upslope accumulated area (UAAB), and topographic position index (TPI). TWI is the log of flow accumulation area divided by slope, and TPI represents the local-scale variation of topography after topographic trend (i.e. the moving average of 100-m scale) is removed (Gillin *et al* 2015). Since solar radiation is known to be important for high-elevation mountain regions (Körner 2007), the annual sum of hourly potential solar radiation (including direct, diffuse, and reflected) was calculated from DEM, based on (Hebeler 2016) and (Kumar *et al* 1997).

For geology, we used the digitized geological map from the USGS National Geologic Map Data Base (Pribulick *et al* 2016). We grouped geological classes into six main classes: shale, igneous rock, alluvial, glacial, landslide, and unconsolidated deposits. Although a soil map was available, it was uniform except for outcrop regions and was thus not informative. We assumed that the geological map and topographic metrics could capture the variability in soil properties, since (Bailey *et al* 2014) and (Gillin *et al* 2015) documented the strong correlations between topographic metrics and soil properties.

Within the RF algorithm, the importance ranking of predictors was created by (1) setting aside a subset of data as a testing set (i.e. out-of-bag data), (2) predicting the drought sensitivity and computing the accuracy (i.e. out-of-bag error), and (3) computing the increase in the mean-squared-errors (MSE) of prediction after permuting each predictor (i.e. randomly assigning the predictor values from the data values). In addition, we created partial dependence plots to visualize the dependence of sensitivity on each predictor. We used R's randomForest package ([cran.r-project.org/web/packages/rpart/index.html](http://cran.r-project.org/web/packages/rpart/index.html)). The number of trees was equal to 800, which was enough to achieve convergence. The number of candidate variables at each split was the number of variables divided by three, and the minimum size of terminal nodes was five.

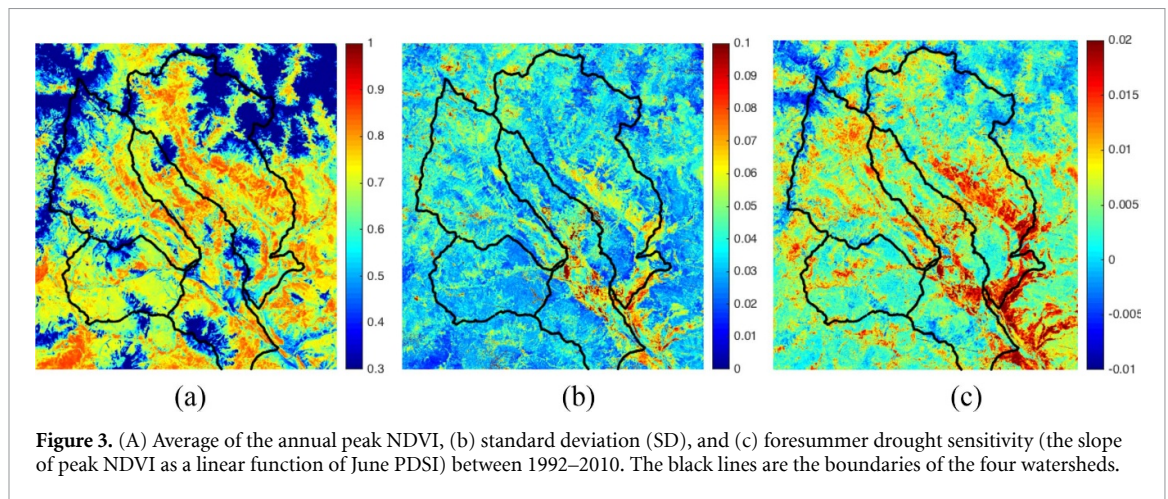
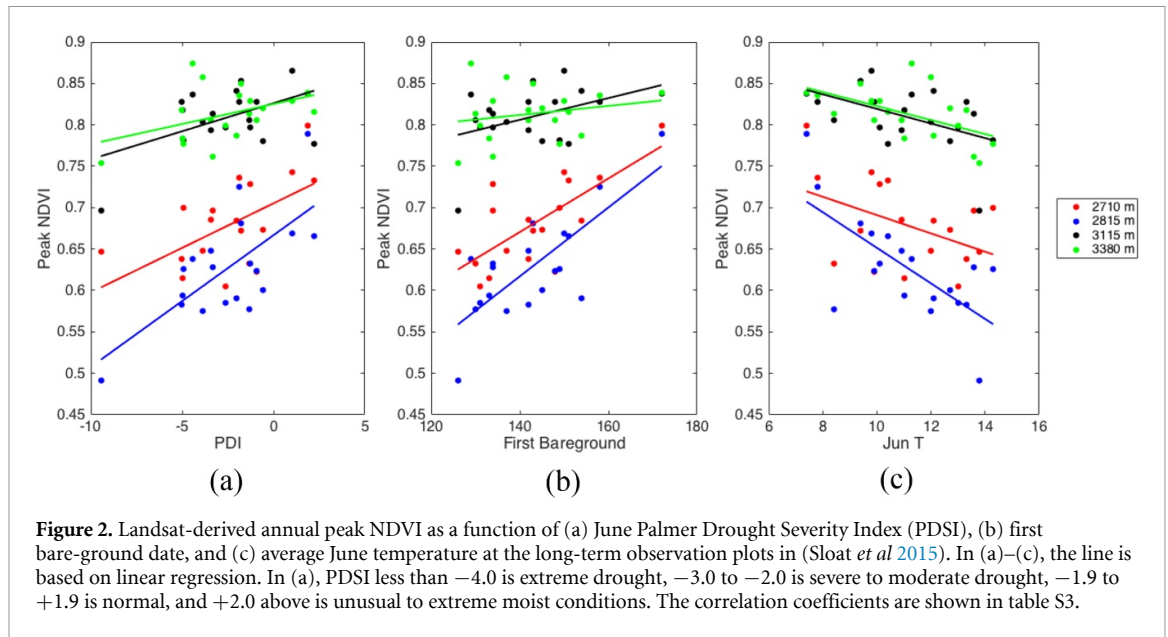
### 3. Results

At the plot locations in (Sloat *et al* 2015), Landsat-derived peak NDVI is positively correlated with June PDSI and snowmelt timing (figures 2(a) and b, table

S3), which is consistent with their findings for peak NEP (note that the data range of PDSI is different because of the differences in the PDSI sources). Increased drought conditions and earlier snowmelt are associated with decreased peak NDVI. Similar to peak NEP, the two subalpine-zone plots (elevation 3115 m and 3380 m) have higher peak NDVI than the montane-zone plots (elevation 2710 m and 2815 m). In addition, peak NDVI is negatively correlated with June mean temperature (June T) at all the locations (figure 2(c) and table S3). These findings are consistent when we use the other drought indices (SPI and SPEI; figure S3) and the linear regression without the extreme years (figure S4). There are some differences between peak NDVI in figure 2 and peak NEP shown in (Sloat *et al* 2015). In figure 2, the slope values of peak NDVI are distinctly different between the subalpine and montane plots. At the subalpine plots, peak NDVI has lower dependency on June PDSI, snowmelt timing, and June T. By contrast, in figure 3 of (Sloat *et al* 2015), the slope values are similar at the four plots.

The average peak NDVI (figure 3(a)) is spatially heterogeneous over the domain, ranging from 0.2 to 0.9 in the vegetated area. The heterogeneity is related to both elevation and vegetation type (figure S5). Within the grassland area (figure S5(a)), the overall trend of peak NDVI increases with elevation up to ~3100 m, and then decreases. The deciduous forest region (i.e. *Populus tremuloides* or aspen) has higher average peak NDVI than the other vegetation types (figure S5(b)). The evergreen forest has lower peak NDVI on average across the watershed (figure S5(c)), and also smaller spatial heterogeneity compared to the other vegetation types. Year-to-year variability of peak NDVI is represented by SD at each pixel (figure 3(b)). The region with the higher average peak NDVI (figure 3(a)) does not necessarily correspond to the one with high SD (figure 3(b)). Higher elevation portions of the East River drainage, for example, have high peak NDVI on average, but low SD.

The foresummer drought sensitivity of peak NDVI (figure 3(c)) is positive in 94.1% of the vegetated area, although it is highly heterogeneous across the domain. Although the sensitivity map is fairly similar to the SD map (figure 3(b)), the spatial heterogeneity of sensitivity is more pronounced than the SD. The southern (or lower elevation) part of the East River watershed (lower elevation and grassland areas) is particularly sensitive to the June drought condition. The northern (or higher elevation) part of the East River watershed has lower sensitivity, although the average peak NDVI is high (figure 3(a)). The spatial heterogeneity of sensitivity depends heavily on plant types and elevation (figure 4). Summary statistics (table S4) show a clear dependency of drought sensitivity on plant types, confirmed by Tukey's pairwise comparison test ( $p$ -values  $< 1 \times 10^{-4}$ ). Grasslands (figure 4(a)) have higher sensitivity than the other



plant types, particularly at lower elevation, and also has larger spatial heterogeneity across the domain. Elevation dependency (figure 4(d)) in the grassland region is much more apparent than in the SD map (figure S6(d)). Evergreen forests exhibit the lowest sensitivity to the foresummer drought, although the sensitivity is still positive in 92.6% of the area. In addition, sensitivity is spatially less heterogeneous without significant elevation dependency (figure 4(f)).

We applied the RF analysis to foresummer drought sensitivity within the grassland region. Although we have the results in other plant types (table S5 and figures S7 and S8), we focus our discussion on the grassland region, because the grassland region has (1) higher spatial heterogeneity than other plant types, (2) the locations corresponding to the long-term plots in (Sloat *et al* 2015), and (3) the ground-based LAI-NDVI relationship (figure S2). The coefficient of determination (R-square) is 0.58, with the  $p$ -value less than  $10^{-15}$ . In the importance ranking (table 1), elevation is the strongest predictor for foresummer drought

**Table 1.** Parameter importance ranking from the random forest analysis; the parameters influencing the spatial heterogeneity of foresummer drought sensitivity within the grassland region. The importance measure (i.e. %MSE) is normalized by one for elevation, so that it represents relative importance compared to elevation. The shaded cells indicate the top four in the importance ranking.

	Normalized %MSE
Elevation	1.00
Slope	0.44
Curvature	0.24
TWI	0.28
Geology	0.56
Radiation	0.63
TPI	0.61
UAAB	0.24

sensitivity, which is consistent with the clear dependency on elevation (figure 4(e)). Net potential radiation, topography position index (TPI), geology, and slope follow in the ranking. The three topographic metrics (TWI, UAAB and curvature) are relatively

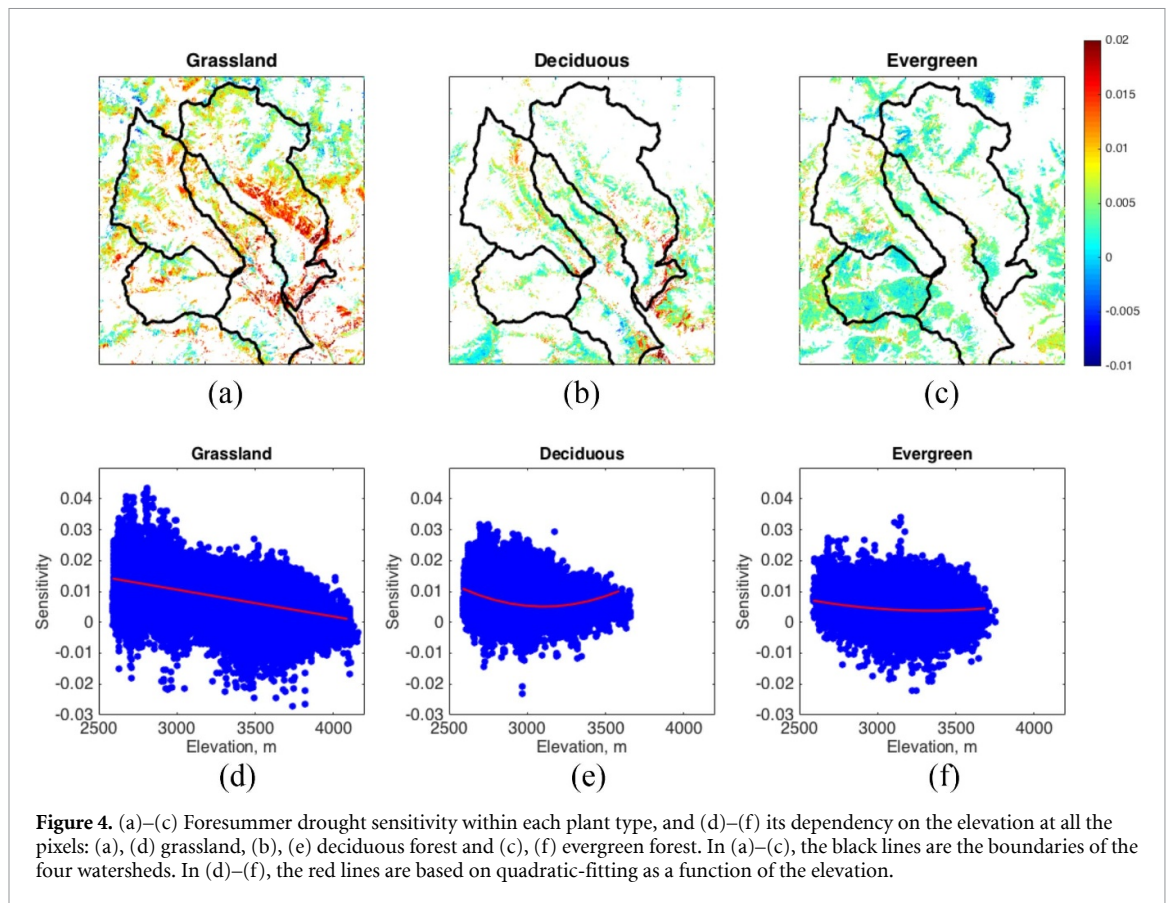


**Figure 4.** (a)–(c) Foresummer drought sensitivity within each plant type, and (d)–(f) its dependency on the elevation at all the pixels: (a), (d) grassland, (b), (e) deciduous forest and (c), (f) evergreen forest. In (a)–(c), the black lines are the boundaries of the four watersheds. In (d)–(f), the red lines are based on quadratic-fitting as a function of the elevation.

weak predictors. In addition, we have analyzed the datasets in different resolutions up to 600 m, which showed the same predictors as the 30 m resolution results (texts 3; table S6).

Partial dependence plots are shown for the top four predictors in the importance ranking (figure 5). The dependency on elevation (figure 5(a)) is approximately linear, which is consistent with the elevation trend in figure 4(d). The dependency on net potential radiation (figure 5(b)) is nonlinear, with the effect more pronounced for the higher radiation regions. The dependency on TPI (figure 5(c)) is close to a step function, such that the regions having higher than the overall elevation gradients (i.e. microtopographically elevated) have higher drought sensitivity. With respect to geology (figure 5(d)), the igneous rock region is associated with decreased drought sensitivity, while glacial, landslide, and unconsolidated deposits are associated with increased sensitivity. We also investigated the correlations among the predictors such as elevation with radiation and aspect (figure S9).

#### 4. Discussion

At the long-term study plots in (Sloat *et al* 2015), the satellite observations of peak NDVI are consistent with peak NEP such that (1) peak NDVI is positively correlated with June PDSI and snowmelt timing, and (2) peak NDVI is greater at the subalpine

plots than at the montane plots. These consistent responses confirm that plant dynamics are water limited in this region and that early snowmelt decreases plant productivity, as suggested by previous studies (Harte *et al* 2015, Sloat *et al* 2015). The subalpine plots are considered less water limited, given deeper snowpack and later snowmelt. In addition, we find that peak NDVI is negatively correlated with average June temperature. Higher June temperature is known to be associated with earlier snowmelt and higher ET (Foster *et al* 2016), which exacerbates the foresummer drought condition and has a negative impact on plant growth.

There are differences between peak NDVI and NEP. While peak NEP responds similarly to June PDSI across the elevation gradient in (Sloat *et al* 2015), satellite-derived peak NDVI is less sensitive at the subalpine plots. This could result from the fact that NDVI represents only aboveground plant dynamics, while NEP includes soil respiration. (Sloat *et al* 2015) found that soil respiration was less affected by watering experiments, suggesting that soil respiration was less sensitive to droughts. Although NDVI has been used for upscaling NEP (e.g. Sturtevant and Oechel 2013), the applications in mountainous regions may not be straightforward, owing to nonlinear responses along the elevational gradient.

We considered the potential effect of the NDVI saturation at the high LAI region. Although this grassland region is not a high biomass region (Gao

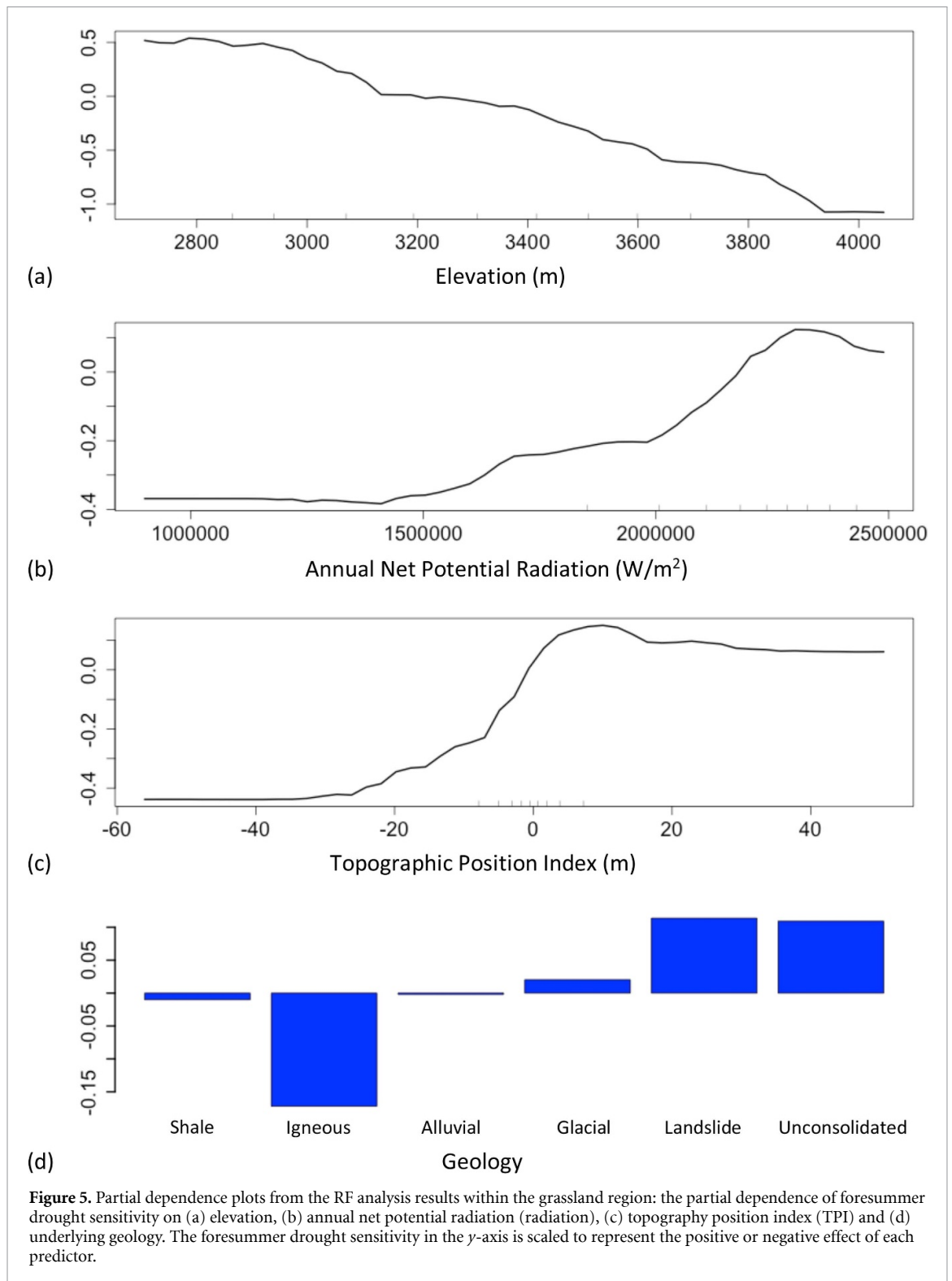


**Figure 5.** Partial dependence plots from the RF analysis results within the grassland region: the partial dependence of foresummer drought sensitivity on (a) elevation, (b) annual net potential radiation (radiation), (c) topography position index (TPI) and (d) underlying geology. The foresummer drought sensitivity in the *y*-axis is scaled to represent the positive or negative effect of each predictor.

*et al 2000, Huete et al 2002, Gu et al 2013*), NDVI at the two high elevation locations (figure 2) are as high as 0.85. In the NDVI-LAI relationship (figure S2), we observe possible saturation in NDVI above ~0.85. We fitted these datasets with a linear and second-order polynomial function for NDVI < 0.85. Since the R<sup>2</sup> and BIC are comparable, we may use the linear function up to NDVI = 0.85. We would note that peak NDVI is less than 0.85 in 92.4% of the domain even

in 1995, when peak NDVI is the highest. In parallel, we considered the potential effect of such saturation on our results. If the effect of the decreased sensitivity were due to NDVI saturation, the sensitivity—defined as the slope of peak NDVI as a function of PDSI—would decrease in high NDVI regions. In figure 4(d), the sensitivity decreases as the elevation increases, while the average peak NDVI (figure S5(d)) also decreases above ~3100 m. Therefore, we

may conclude that the decreased sensitivity at high elevation does not result from the saturation effect. In addition, we examined the correlation between sensitivity and average peak NDVI, which was not significant (correlation coefficient of  $-0.026$ ).

Satellite-derived NDVI allows us to extend our plot-scale understanding to the watershed scale. Landsat 5 has provided long-term historical images at high-enough resolution to distinct plant types and gauge the effect of topography and geology on sensitivity. In the subalpine zone (around 3000–3300 m), peak plant productivity is high on average, and has small interannual variability without significant dependency on the regional-scale June PSDI, possibly because this zone has more snow and water compared to lower elevations. In addition, our results show that the magnitude and spatial variability of drought sensitivity is clearly dependent on plant type, with the grassland regions having higher sensitivity and higher spatial heterogeneity. This dependency on plant type is considered to result from rooting depth as well as geographic location—evergreen trees tend to occupy north-facing slopes that have more snow accumulation and higher soil moisture. At the same time, forest drought sensitivity is predominantly positive within the evergreen forest regions, suggesting that the increased drought severity—due to early snowmelt and/or increased spring temperature—would decrease forest productivity, which is consistent with a basin-scale study by (Knowles *et al* 2018). In addition, we observe that 6% of the region, primarily at high elevation, has increased peak NDVI in drought years. It suggests that the high elevation regions are temperature-limited rather than water-limited. This is consistent with (Dong *et al* 2019), which found that MODIS-based NDVI increased at higher elevation in drought years.

In this study, we defined the foresummer drought sensitivity by the slope of the linear regression between peak NDVI and June PSDI. With respect to sensitivity measures, there are slope-based and variance-based measures in general to represent sensitivity (e.g. Morris 1991, Saltelli *et al* 2008, Wainwright *et al* 2014). Several studies have used variance or variance-based metrics to represent ecosystem sensitivities (e.g. Seddon *et al* 2016). In our results, we find that the slope-based sensitivity measure is more informative in this type of analyses, since we can identify positive or negative changes associated with foresummer drought conditions.

We consider that PSDI and other drought indices (such as PSI and SPEI) represent the regional-scale climatic variability being driven by precipitation and temperature. Vicente-Serrano *et al* (Vicente-Serrano *et al* 2012) found that ecosystem responses (i.e. tree-ring growth and wheat yield) to droughts were captured by SPEI, as well as other drought indices. In our analysis, the response of peak NDVI was consistent to each other among these three

drought indices (PSDI, PSI, SPEI), confirming the impact of water limitation on plant productivity over this region. At the same time, we highlight that this study focuses on the spatial variability of foresummer drought sensitivity at the local-scale (30 m), so that we can resolve the effect of topography, plant type, and geology. While these local-scale environmental characteristics could be viewed as secondary factors, recent studies have found that such characteristics (e.g. geology) are important for subsurface water storage (Markovich *et al* 2016) and the resilience of ecosystems (Rempe and Dietrich 2018).

The RF analysis enables us to identify key environmental controls on foresummer drought sensitivity within each plant cover type. Elevation and net radiation are the two most dominant factors, possibly because they control surface energy balance and snow accumulation and melting. We would note that the higher-elevation hillslopes tend to be north-facing in our domain, which could amplify the effect of reduced drought sensitivity in high-elevation regions. The topography position index (i.e. indicator of microtopography) and slope are known to control soil moisture (Mohanty *et al* 2000, Gillin *et al* 2015). Falco *et al* (2019) found a significant correlation between slope and soil moisture in the grassland regions within this domain. In addition, the results show the importance of underlying geologic composition on drought sensitivity. Well-drained soil developed upon glacial and landslides deposits are likely to shed near-surface soil moisture (associated with plant rooting) rapidly after snowmelt. In contrast, the region underlain by shale and igneous rocks has lower drought sensitivity. Rempe *et al* (2018) found that fractured bedrock can retain water during droughts and is less affected by year-to-year variability. Having shallow bedrock may provide resilience to droughts.

This study used publicly available PSDI and Landsat data to estimate foresummer drought sensitivity of peak plant productivity in headwater catchments. We did not explicitly include other datasets, for example, the spatial distribution of snow accumulation/snowmelt and precipitation, since these factors are difficult to map in space and time (Lettenmaier *et al* 2015). Instead, we assumed that the topographic metrics are reflective of snow and precipitation patterns, given that the effects of topography on these patterns have been well documented in many studies (e.g. Anderson *et al* 2014). Both these assumptions, and our approach, open the door for upscaling plot-scale analyses and understandings to a large area, using publicly available datasets. We acknowledge that the overlapping coverage of Landsat paths was advantageous for our domain to minimize the impact of cloud coverage. At the same time, our analysis based on different spatial resolutions found that the effects of key drivers (i.e. elevation and radiation) were consistent up to the resolution of

several hundred meters, which would suggest that we may use lower-resolution high-frequency satellites such as MODIS. Remote-sensing-derived drought sensitivity can be a useful metric for identifying the regions that are resilient or vulnerable to climate perturbations and long-term climatic shifts, as well as for identifying key underlying processes.


## Acknowledgments

This material is based upon work supported by the U.S. Department of Energy, Office of Science, Office of Biological and Environmental Research, Earth and Environmental Systems Sciences Division and Data Management Program, under Award Number DE-AC02-05CH11231, as part of the Watershed Function Scientific Focus Area and the ExaShed project. Sarah Trutner was supported by the U.S. Department of Energy, Office of Science, Office of Workforce Development for Teachers and Scientists under the Science Undergraduate Laboratory Internship program. E I Nikolopoulos was supported by the US National Science Foundation under Grant No. 1934712. We thank two anonymous reviewers for constructive comments.

## Data Availability Statement

The data that support the findings of this study are openly available. All the datasets in this study are publicly available through the data source specified in the manuscript.

## ORCID iDs

Haruko M Wainwright  <https://orcid.org/0000-0002-2140-6072>

K Dana Chadwick  <https://orcid.org/0000-0002-5633-4865>

## References

- U.S. Geological Survey 2002 *National Elevation Dataset* (available at: [ned.usgs.gov](http://ned.usgs.gov))
- Alley W M 1984 The Palmer drought severity index: limitations and assumptions *J. Clim. Appl. Meteorol.* **23** 1100–9
- Anderson B T, Mcnamara J P, Marshall H P and Flores A N 2014 Insights into the physical processes controlling correlations between snow distribution and terrain properties *Water Resour. Res.* **50** 4545–63
- Bachmair S and Weiler M 2012 Hillslope characteristics as controls of subsurface flow variability *Hydrol. Earth Syst. Sci.* **16** 3699–715
- Bailey S, Brousseau P, Mcguire K and Ross D 2014 Influence of landscape position and transient water table on soil development and carbon distribution in a steep, headwater catchment *Geoderma* **226** 279–89
- Beguéria S, Vicente-Serrano S M and Angulo M 2010 A multi-scalar global drought data set: the SPEIbase: A new gridded product for the analysis of drought variability and impacts *Bull. Am. Meteorol. Soc.* **91** 1351–4
- Berner L T, Law B E and Hudiburg T W 2017 Water availability limits tree productivity, carbon stocks, and carbon residence time in mature forests across the western US *Biogeosciences* **14** 365–78
- Breiman L 2001 Random forests *Mach. Learn.* **45** 5–32
- Carroll R, Bearup L, Brown W, Dong W, Bill M and Williams K 2018 Factors controlling seasonal groundwater and solute flux from snow-dominated basins *Hydrol. Process.* **32**
- Dai A, Trenberth K E and Qian T 2004 A global dataset of palmer drought severity index for 1870–2002: relationship with soil moisture and effects of surface warming *J. Hydrometeorol.* **5** 1117–30
- De Jong R, de Bruin S, de Wit A, Schaeppman M and Dent D 2011 Analysis of monotonic greening and browning trends from global NDVI time-series *Remote Sens. Environ.* **115** 692–702
- Diffenbaugh N S, Scherer M and Ashfaq M 2013 Response of snow- dependent hydrologic extremes to continued global warming *Nat. Clim. Change* **3** 379–84
- Dong C, Macdonald G M, Willis K, Gillespie T W, Okin G S and Williams A P 2019 Vegetation responses to 2012–2016 drought in Northern and Southern California *Geophys. Res. Lett.* **46** 3810–21
- Ernakovich J, Hopping K, Berdanier A, Simpson R, Kachergis E, Steltzer H and Wallenstein M 2014 Predicted responses of arctic and alpine ecosystems to altered seasonality under climate change *Glob. Change Biol.* **20** 3256–69
- Euskirchen E S et al 2006 Importance of recent shifts in soil thermal dynamics on growing season length, productivity, and carbon sequestration in terrestrial high-latitude ecosystems *Glob. Change Biol.* **12** 731–50
- Falco N, Wainwright H, Dafflon B, Léger E, Peterson J, Steltzer H, Wilmer C, Rowland J C, Williams K H and Hubbard S S 2019 Investigating microtopographic and soil controls on a mountainous meadow plant community using high-resolution remote sensing and surface geophysical data *J. Geophys. Res. Biogeosci.* **124** 1618–36
- Foster L M and Maxwell R M 2019 Sensitivity analysis of hydraulic conductivity and Manning's n parameters lead to new method to scale effective hydraulic conductivity across model resolutions *Hydrol. Process.* **33** 332–49
- Foster L, Bearup L, Molotch N, Brooks P and Maxwell R 2016 Energy budget increases reduce mean streamflow more than snow–rain transitions: using integrated modeling to isolate climate change impacts on Rocky Mountain hydrology *Environ. Res. Lett.* **11** 044015
- Gao X, Huete A R, Ni W and Miura T 2000 Optical–biophysical relationships of vegetation spectra without background contamination *Remote Sens. Environ.* **74** 609–20
- Gillin C, Bailey S, Mcguire K and Gannon J 2015 Mapping of Hydropedologic Spatial Patterns in a Steep Headwater Catchment *Soil Sci. Soc. Am. J.* **79** 440
- Gu Y, Wylie B K, Howard D M, Phuyal K P and Ji L 2013 NDVI saturation adjustment: A new approach for improving cropland performance estimates in the Greater Platte River Basin, USA *Ecol. Indic.* **30** 1–6
- Harte J, Saleska S and Levy C 2015 Convergent ecosystem responses to 23-year ambient and manipulated warming link advancing snowmelt and shrub encroachment to transient and long-term climate–soil carbon feedback *Glob. Change Biol.* **21** 2349–56
- Hastie T, Tibshirani R and Friedman J H 2001 *The Elements of Statistical Learning: Data Mining, Inference, and Prediction* (Berlin: Springer) (<https://doi.org/10.1007/978-0-387-84858-7>)
- Hebeler F 2016 *Matlab File Exchange: Solar Radiation* ([www.mathworks.com/matlabcentral/fileexchange/19791-solar-radiation/content/solarradiation.m](http://www.mathworks.com/matlabcentral/fileexchange/19791-solar-radiation/content/solarradiation.m))
- Higgins R W and Shi W 2001 Intercomparison of the principal modes of interannual and intraseasonal variability of the North American monsoon system *J. Clim.* **14** 403–17

- Hubbard S S *et al* 2018 The East River, Colorado, Watershed: A mountainous community testbed for improving predictive understanding of multiscale hydrological–biogeochemical dynamics *Vadose Zone J.* **17** 1–25
- Huete A, Didan K, Miura T, Rodriguez E P, Gao X and Ferreira L G 2002 Overview of the radiometric and biophysical performance of the MODIS vegetation indices *Remote Sens. Environ.* **83** 195–213
- Kim Y, Kimball J S, Zhang K and McDonald K C 2012 Satellite detection of increasing Northern Hemisphere non-frozen seasons from 1979 to 2008: implications for regional vegetation growth *Remote Sens. Environ.* **121** 472–87
- Knowles J F, Lestak L R and Molotch N P 2017 On the use of a snow aridity index to predict remotely sensed forest productivity in the presence of bark beetle disturbance *Water Resour. Res.* **53** 4891–906
- Knowles J F, Molotch N P, Trujillo E and Litvak M E 2018 Snowmelt-driven trade-offs between early and late season productivity negatively impact forest carbon uptake during drought *Geophys. Res. Lett.* **45** 3087–96
- Kumar L, Skidmore A K and Knowles E 1997 Modelling topographic variation in solar radiation in a GIS environment *Int. J. Geogr. Info. Sys.* **11** 475–97
- Körner C 2007 The use of ‘altitude’ in ecological research *Trends Ecol. Evol. (Amst.)* **22** 569–74
- Lamanna C A 2012 The structure and function of subalpine ecosystems in the face of climate change *PhD Dissertation*, University of Arizona
- Lettenmaier D, Alsdorf D, Dozier J, Huffman G, Pan M and Wood E 2015 Inroads of remote sensing into hydrologic science during the WRR era *Water Resour. Res.* **51** 7309–42
- Lukas J, Barsugli J, Doesken N, Rangwala I and Wolter K 2015 *Climate Change in Colorado: A Synthesis to Support Water Resources Management and Adaptation* 2nd edn (Boulder, CO: Western Water Assessment, Cooperative Institute for Research in Environmental Sciences (CIRES))
- Markovich K, Maxwell R and Fogg G 2016 Hydrogeological response to climate change in alpine hillslopes *Hydrol. Process.* **30** 3126–38
- Maxwell R M and Condon L E 2016 Connections between groundwater flow and transpiration partitioning *Science* **353** 377–80
- Mckee T B N, Doesken J and Kleist J, 1993 The relationship of drought frequency and duration to time scales *Proc. Eight Conf. on Applied Climatology. Anaheim, CA, Amer. Meteor. Soc.* pp 179–84
- Mohanty B P, Famiglietti J S and Skaggs T H 2000 Evolution of soil moisture spatial structure in a mixed vegetation pixel during the Southern Great Plains 1997 (SGP97) hydrology experiment *Water Resour. Res.* **36** 3275–86
- Morris M D 1991 Factorial sampling plans for preliminary computational experiments *Technometrics* **33** 161–74
- Oyler J W, Dobrowski S Z, Ballantyne A P, Klene A E and Running S W 2015 Artificial amplification of warming trends across the mountains of the western United States *Geophys. Res. Lett.* **42** 153–61
- Painter T H, Berisford D F and Boardman J W 2016 The airborne snow observatory: fusion of scanning lidar, imaging spectrometer, and physically-based modeling for mapping snow water equivalent and snow albedo *Remote Sens. Environ.* **184** 139–52
- Pribulick C, Foster L, Bearup L, Navarre-Sitchler A, Williams K, Carroll R and Maxwell R 2016 Contrasting the hydrologic response due to land cover and climate change in a mountain headwaters system *Ecohydrology* **9** 1431–8
- Rauscher S A, Giorgi F, Diffenbaugh N S and Seth A 2008 Extension and intensification of the Meso-American mid-summer drought in the twenty-first century *Clim. Dyn.* **31** 551–71
- Rempe D M and Dietrich W E 2018 Direct observations of rock moisture, a hidden component of the hydrologic cycle *Proc. Natl Acad. Sci.* **115** 2664–9
- Saltelli A, Ratto M, Andres T, Campolongo F, Cariboni J, Gatelli D, Saisana M and Tarantola S 2008 *Global Sensitivity Analysis: The Primer* (New York: Wiley) (<https://doi.org/10.1002/9780470725184>)
- Schwanghart W and Kuhn N J 2010 TopoToolbox: A set of Matlab functions for topographic analysis *Environ. Model. Softw.* **25** 770–81
- Seddon A W, Macias-Fauria M, Long P R, Benz D and Willis K J 2016 Sensitivity of global terrestrial ecosystems to climate variability *Nature* **531** 229–32
- Seth A, Rauscher S A, Rojas M, Giannini A and Camargo S J 2011 Enhanced spring convective barrier for monsoons in a warmer world? *Clim. Change* **104** 403–14
- Sloat L, Henderson A, Lamanna C and Enquist B 2015 The effect of the foresummer drought on carbon exchange in subalpine meadows *Ecosystems* **18** 533–45
- Stocker B D, Zscheischler J, Keenan T F, Prentice I C, Seneviratne S I and Peñuelas J 2019 Drought impacts on terrestrial primary production underestimated by satellite monitoring *Nat. Geosci.* **12** 264
- Sturtevant C S and Oechel W C 2013 Spatial variation in landscape-level CO<sub>2</sub> and CH<sub>4</sub> fluxes from arctic coastal tundra: influence from vegetation, wetness, and the thaw lake cycle *Glob. Change Biol.* **19** 2853–66
- Swain S and Hayhoe K 2015 CMIP5 projected changes in spring and summer drought and wet conditions over North America *Clim. Dyn.* **44** 2737–50
- Trenberth K E, Dai A, van der Schrier G, Jones P D, Barichivich J, Briffa K R and Sheffield J 2014 Global warming and changes in drought *Nat. Clim. Change* **4** 17–22
- Tucker C J, Vanpraet C L, Sharman M J and Van Ittersum G 1985 Satellite remote sensing of total herbaceous biomass production in the senegalese sahel: 1980–1984 *Remote Sens. Environ.* **17** 233–49
- Vicente-Serrano S M, Beguería S, Lorenzo-Lacruz J, Camarero J J, López-Moreno J J, Azorin-Molina C, Revuelto J, Morán-Tejeda E and Sanchez-Lorenzo A 2012 Performance of drought indices for ecological, agricultural, and hydrological applications *Earth Interact.* **16** 1–27
- Wainwright H M, Finsterle S, Jung Y, Zhou Q and Birkholzer J T 2014 Making sense of global sensitivity analyses *Comput. Geosci.* **65** 84–94
- Williams A *et al* 2012 Temperature as a potent driver of regional forest drought stress and tree mortality *Nat. Clim. Change* **3** 292–7
- Zhao M S and Running S W 2010 Drought-Induced reduction in global terrestrial net primary production from 2000 through 2009 *Science* **329** 940–3
- Zimmermann N and Kienast F 1999 Predictive mapping of alpine grasslands in Switzerland: species versus community approach *J. Veg. Sci.* **10** 469–82